JGR Atmospheres

RESEARCH ARTICLE
10.1029/2020JD033039

Multiple-Stroke Positive Cloud-to-Ground Lightning Observed by the FALMA in Winter Thunderstorms in Japan

Ting Wu[1], **Daohong Wang**[1], **and Nobuyuki Takagi**[1]

[1]Department of Electrical, Electronic and Computer Engineering, Gifu University, Gifu, Japan

Key Points:
- Forty-seven multi-stroke +CG flashes containing two to five positive strokes observed in winter thunderstorms in Japan are analyzed
- Interstroke intervals, distances between sequential strokes and peak amplitudes of first and subsequent strokes are statistically analyzed
- Positive leaders initiating most subsequent strokes are originated from in-cloud negative leader channels

Supporting Information:
- Supporting Information S1

Correspondence to:
T. Wu,
tingwu@gifu-u.ac.jp

Citation:
Wu, T., Wang, D., & Takagi, N. (2020). Multiple-stroke positive cloud-to-ground lightning observed by the FALMA in winter thunderstorms in Japan. *Journal of Geophysical Research: Atmospheres*, *125*, e2020JD033039. https://doi.org/10.1029/2020JD033039

Received 1 MAY 2020
Accepted 23 SEP 2020
Accepted article online 30 SEP 2020

Abstract Multiple-stroke (MS) positive cloud-to-ground (+CG) lightning flashes are rarely reported, especially those with high-quality location information. In this study, we report 47 MS +CG flashes observed in winter thunderstorms in Japan with a 14-site fast antenna lightning mapping array (FALMA). MS +CG flashes account for 18% of +CG flashes. The mean multiplicity of all +CG flashes is 1.24, and the maximum multiplicity is 5. Interstroke intervals have a very large range from 1.0 to 1,320.6 ms with the geometric mean of 64.4 ms. In three flashes, interstroke intervals smaller than 2 ms are observed, and corresponding positive strokes are inferred to be produced by two branches of the same positive leader. Horizontal distances between sequential positive strokes range from 1.1 to 37.3 km with the geometric mean of 9.7 km. No subsequent strokes struck at the same location as a previous stroke. Distances between sequential strokes are generally much larger than distances between first strokes and lightning initiation locations. Subsequent stroke peak amplitudes are on average 0.45 of first stroke peak amplitudes. In 39 flashes (83%), the first stroke is stronger than the largest subsequent stroke in the same flash. Subsequent stroke amplitudes are weakly correlated with the time difference from the previous stroke. Origination mechanisms of positive leaders initiating first and subsequent positive strokes are discussed. It is very likely that positive leaders for most subsequent strokes originate from in-cloud negative leader channels, but origination mechanisms for positive leaders initiating first strokes are more varied.

1. Introduction

Positive cloud-to-ground (+CG) lightning flashes are usually much less frequent than negative CG (−CG) flashes. It is estimated that less than 10% of CG flashes globally are positive flashes (e.g., Rakov, 2003). However, positive return strokes (RSs) are more likely to carry extremely large peak currents (e.g., Lyons et al., 1998) and thus pose particular threats to various objects. It is also well known that transient luminous events such as sprites are almost always associated with +CG flashes (e.g., Williams et al., 2007). Therefore, +CG flashes have attracted considerable research interest in recent years.

An interesting feature of +CG lightning that is not well understood is that most +CG flashes contain only one RS. Multiple-stroke (MS) +CG flashes do occur but are uncommon. Table 1 summarizes studies reporting MS +CG flashes, and we can see that the percentage of MS +CG flashes relative to all +CG flashes is generally from 10% to 20%. As a result, high-quality data of MS +CG flashes are extremely difficult to obtain. In fact, most studies summarized in Table 1 were based on electric field records and/or nationwide lightning location systems, from which it is even difficult to unambiguously determine whether two RSs belong to the same flash.

Although +CG flashes are generally rare, they are more frequent in some situations as reviewed by Rakov (2003). One of the situations is winter thunderstorms. Based on the observation in one winter season in the Hokuriku region in Japan, we recorded 47 MS +CG flashes, the largest sample reported so far. These flashes were recorded by a low-frequency (LF) lightning mapping system called fast antenna lightning mapping array (FALMA), with which we can obtain electric field change (*E* change) waveforms at multiple sites and image lightning channel developments with great detail. With this high-quality data set, we will clarify some basic properties of MS +CG flashes and will investigate the origination mechanism of positive leaders for first and subsequent strokes in MS +CG flashes.

Table 1
Summary of Studies on MS +CG Flashes

Study	MS +CGs		Multiplicity		Interstroke interval (ms)			Horizontal distance (km)			A_{sub}/A_{1st}[a]
	Number	%	Mean	Maximum	Range	AM	GM	Range	AM	GM	
Present study	47	18	1.24	5	1.0–1320.6[b]	122.2	64.4	1.1–37.3	13.1	9.7	0.45
Cooray & Pérez (1994)	29[c]				6.8–290	92	64				
Heidler & Hopf (1998)	12	27		4		120	101				
Qie et al. (2002)	3	13	1.13	2							
Fleenor et al. (2009)	9	4	1.04	2	13–155			0–			0.74
Saba et al. (2010)	20	19	1.20	3	14–406	143	94	0–53	12.3	11.8	0.73
Nag & Rakov (2012)	10	19	1.21	3	8.5–201	77	54	0.22–29			
Qie et al. (2013)	10	5	1.06	3	6.5–290.7	97.8	64.2				
Adhikari et al. (2016)	11	8	1.10	4	0.3–80.3	33.8	16.7				
Baharudin et al. (2016)	40	37	1.50	4	2.9–518	116	70				0.48[d]
Hazmi et al. (2017)	13	17	1.18	3	16–458	163.9	113.3				0.29[d]
Johari et al. (2017)	6	12	1.20	4	25–124	71	60	4.9–46.4			0.46
Wu et al. (2018a)	7	15	1.15	2							

[a]Ratio of mean peak amplitude of subsequent strokes to that of first strokes. [b]Excluding the extreme case with the value of 1,320.6 ms, the range is 1.0–469.2 ms, the AM is 103.2 ms, and the GM is 61.4 ms. [c]Stroke number. [d]Mean value of the ratio of peak amplitudes of subsequent strokes to those of first strokes.

2. Observation and Data

Winter lightning observation was carried out in the Hokuriku region of Japan from December 2018 to March 2019. A FALMA system consisting of 14 sites was set up as shown in Figure 1. The FALMA is a three-dimensional (3-D) lightning mapping system working in the low-frequency band. Lightning radiation signals are received by a fast antenna with a time constant of 200 μs at each site, and 3-D source locations are calculated with an improved time-of-arrival method. Details about the summer observation with the FALMA in Gifu, Japan, can be found in Wu et al. (2018b).

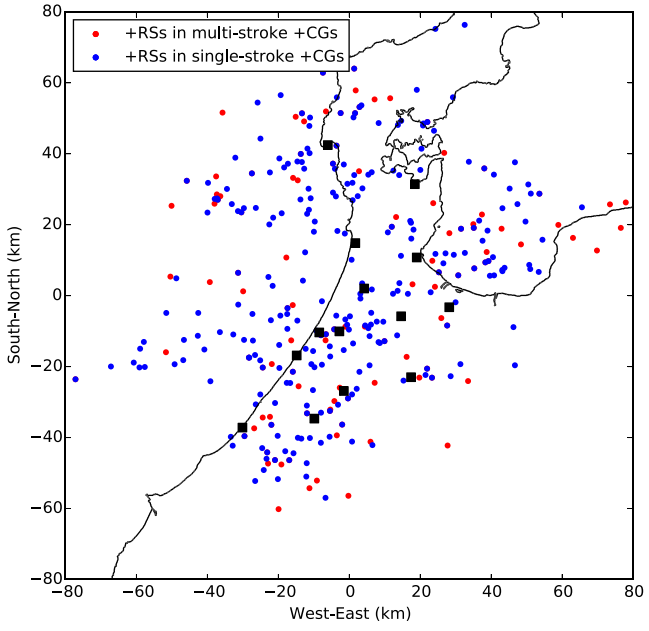

Figure 1. Locations of positive RSs observed during the winter observation in Hokuriku region of Japan. Red dots represent RSs in MS +CGs, and blue dots represent RSs in single-stroke +CGs. Black squares represent 14 sites of the FALMA. The origin (0, 0) corresponds to the latitude and longitude of (36.76°N, 136.76°E).

2.1. Data

Only +CG flashes whose leader channels are mainly within about 60 km from the center of the FALMA network are selected for this study to ensure that at least 2-D mapping of leader channels and localization of RSs can be made accurately. As a result, a total of 263 +CG flashes is identified from the data obtained during the winter, including 216 single-stroke +CG flashes and 47 MS +CG flashes. These +CG flashes produced 327 positive RSs. Locations of these positive RSs are shown in Figure 1 with red dots representing RSs in MS +CG flashes, and blue dots representing RSs in single-stroke +CG flashes.

Eleven of these MS +CG flashes are actually bipolar flashes; they also contain at least one negative RS. In six cases, all negative RSs occurred after all positive RSs. In one case, a negative RS occurred before the first positive RS. In another case, one negative RS occurred before and another after all positive RSs. For these cases, it is assumed that occurrences of negative RSs do not influence most analyses in this study, so these flashes are analyzed as normal MS +CG flashes. In the remaining three cases, one or two negative RSs occurred between two positive RSs. One case has an extremely long interstroke interval and is analyzed separately in section 3.2. The other two cases do not seem to have any special characteristics and are analyzed as normal MS +CG flashes for simplicity.

Figure 2 shows distributions of daily numbers of single-stroke and MS +CG flashes. It is clear that MS +CG flashes are generally produced in the same periods as single-stroke +CG flashes. It is also clear from Figure 1 that MS +CG flashes are produced in the same area as single-

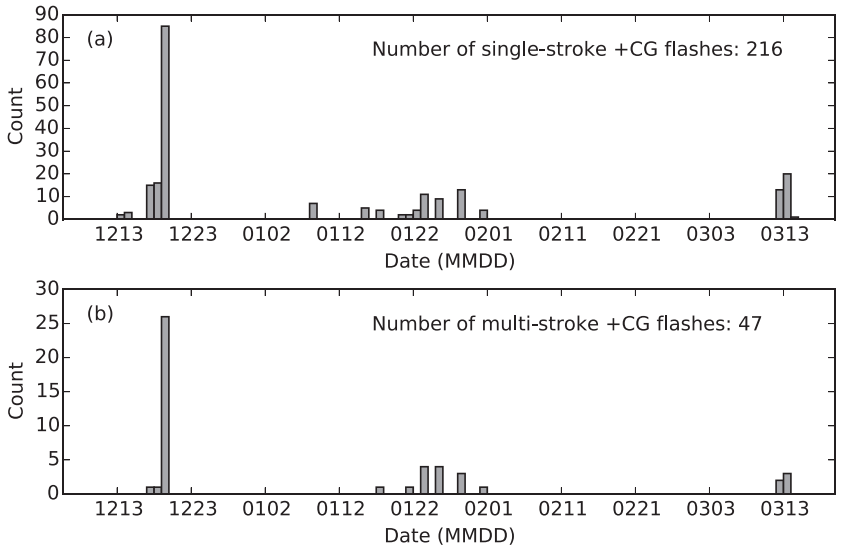

Figure 2. Distributions of daily numbers of (a) single-stroke +CGs and (b) MS +CGs.

stroke +CG flashes. Therefore, it seems that MS +CG flashes are produced in the same thunderstorm conditions as single-stroke +CG flashes.

The atmospheric electricity sign convention is used in this paper, so a positive RS produces a negative E change pulse.

2.2. Evaluation of the Location Accuracy

The FALMA for this study has different site number and baseline distances and is set up in an entirely different area from that used in our summer observation (Wu et al., 2018b). Additionally, lightning discharges in winter have some special characteristics that may also influence the location accuracy. Therefore, it is necessary to have an evaluation of the location accuracy for the FALMA in this study.

Similar to the method used by Wu et al. (2018b), we identified 206 −CG flashes with at least two RSs in the same area as Figure 1 and calculated distances between sequential RSs in the same −CG flash. There were 763 RSs in these −CG flashes, and a total of 557 results of distances between sequential RSs was obtained. Distributions of the distances are shown in Figure 3. Figure 3a shows the distribution for distances smaller than 2,000 m (457 results), and Figure 3b shows the distribution for distances smaller than 500 m (315 results). Locations of these results are shown as points in Figure 3c with the color indicating the distance. Apparently part of the results in Figure 3 are due to −CG flashes with multiple terminations, but it is difficult to determine which of them are due to multiple terminations and which of them are due to location errors. However, from Figure 3 we can get a general picture that the location accuracy for RSs in this area is basically better than 200 m but the accuracy for RSs outside of the network of observation sites can be lower.

Using the same method, Wu et al. (2018b) showed that the distances between sequential RSs in −CGs are mostly smaller than 25 m during the summer observation in Gifu, Japan. The much lower accuracy in this study is due to several possible reasons. One apparent reason is that the evaluation above includes RSs tens of kilometers from the observation network, while the evaluation by Wu et al. (2018b) only considered RSs inside the network. Indeed, from Figure 3c we can see RSs with very large distances from previous strokes are mostly outside of the observation network. Second, the complex topography in this area may have contributed to the low accuracy (e.g., Li et al., 2016). As can be seen in Figure 3c, there are mountain areas both inside and outside of the observation network as well as large sea areas nearby. Another possible reason is that RSs in winter may be more complicated than those in summer, resulting in lower location accuracy. We have seen many peculiar waveforms produced by RSs in winter, but the effect on location accuracy is not well understood so far.

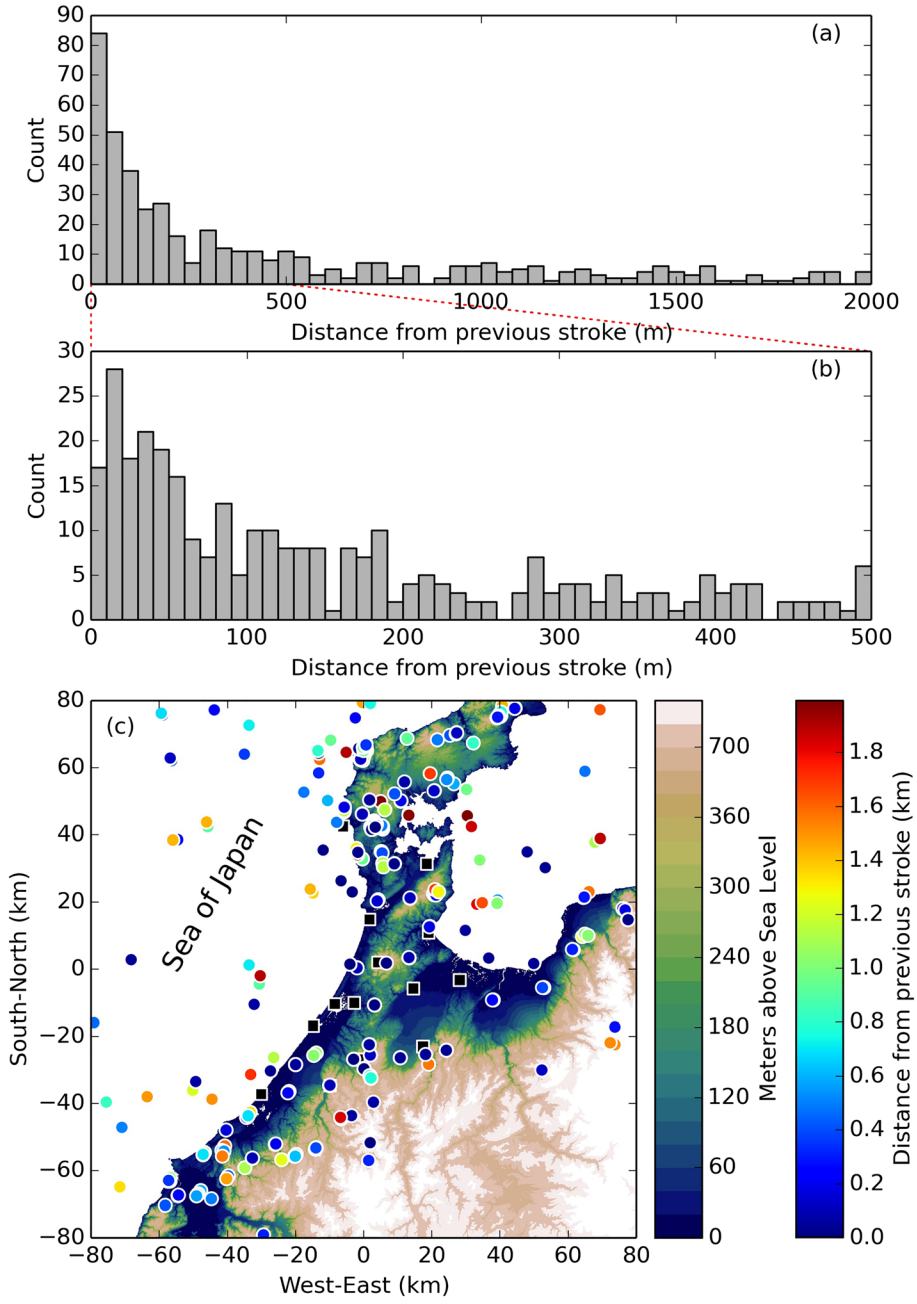

Figure 3. Distances from previous strokes for negative RSs in −CG flashes. (a) Distribution of the distances in the range of 0 to 2,000 m. (b) Distribution of the distances in the range of 0 to 500 m. (c) Locations of the analyzed negative RSs with the color indicating distances from previous strokes.

During the summer observation, we were able to do high-quality 3-D imaging of lightning flashes and infer charge structures of thunderstorms (Wu et al., 2020). However, 3-D imaging in winter seems to be very difficult. According to our analysis of the winter data so far, it seems that only some simple processes (such as upward negative leaders from high objects) at the right locations (surrounded by multiple observation sites) can be well imaged in 3-D. One important reason for the difficulty in 3-D imaging in winter is that lightning discharges in winter generally have much lower altitudes than those in summer. In fact, the lightning mapping array, which works in the VHF band, also seems to have similar difficulties when imaging winter lightning (e.g., Figures 7 and 8 in Schultz et al., 2018). Therefore, height results of MS +CG flashes analyzed in this study are generally considered not reliable, and only 2-D location results will be used.

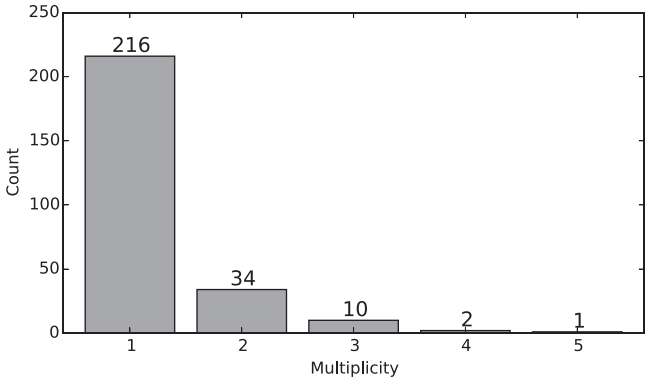

Figure 4. Distribution of the multiplicity of positive RSs in +CGs.

3. Results

3.1. Return Stroke Multiplicity

The distribution of multiplicity of positive RSs in +CG flashes is shown in Figure 4. There are 216 single-stroke flashes, 34 two-stroke flashes, 10 three-stroke flashes, 2 four-stroke flashes, and 1 five-stroke flash. A total of 327 positive RSs was produced by 263 +CG flashes, corresponding to an average of 1.24 strokes per flash.

Mean multiplicities reported by previous studies are summarized in Table 1. The mean multiplicity of 1.24 in this study is larger than all but one previous studies. However, the mean multiplicity reported by several studies are around 1.20 (Hazmi et al., 2017; Johari et al., 2017; Nag & Rakov, 2012; Saba et al., 2010), very close to the current study. If we consider the percentage of MS +CG flashes relative to all +CG flashes, the percentage in this study (18%) is just about the average level of other studies summarized in Table 1. Therefore, although winter thunderstorms in Japan have a clear tendency to produce more frequent +CG flashes, these +CG flashes do not seem to have a higher chance to produce multiple strokes.

The maximum multiplicity in this study is 5. MS +CG flashes containing more than three positive RSs are rarely reported (Lang et al., 2017; Lyons et al., 2020; Soula et al., 2010). This five-stroke flash is shown in Figure 5. Figure 5a shows the plan view of the location results of the flash with the red diamond representing the initiation location and black triangles representing positive RSs. Figure 5b shows the distance-time view (relative to the initiation location and time) similar to the analysis made by van der Velde and Montanyà (2013), and Figure 5c shows the E change waveform recorded at one site. E change waveforms of the five strokes recorded by all sites are shown in Figures S1–S5 in the supporting information. This flash has a large horizontal extent of about 50 × 30 km. The duration of the flash is about 900 ms. Sources of this flash superimposed on the radar reflectivity are shown in Figure S6.

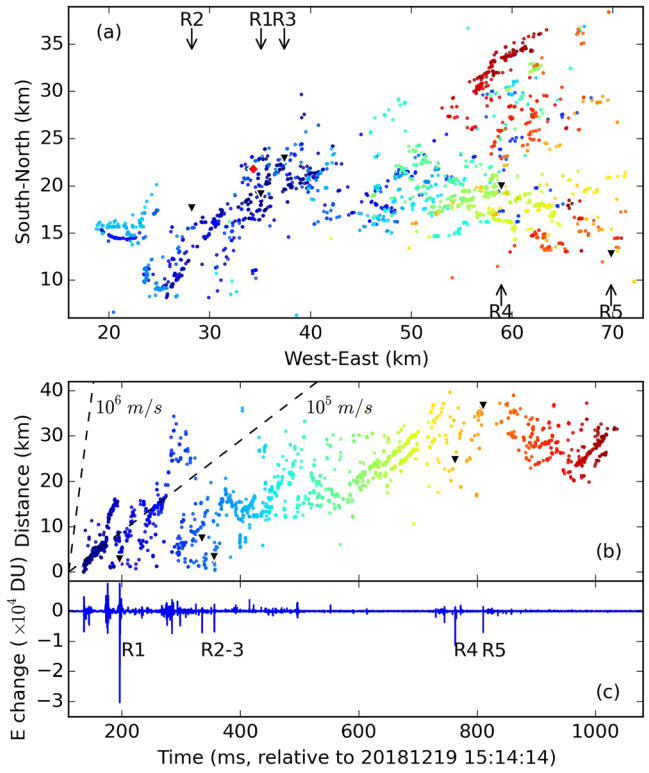

Figure 5. The +CG flash with five positive RSs. (a) Plan view. (b) Horizontal distance (relative to the initiation location) versus time. (c) E change waveform. The red diamond represents the initiation location. Black triangles represent positive RSs. The color scale of source points indicates the time corresponding to the time coordinate of Figure 5c. Slopes of two black dashed lines represent velocities of 10^5 and 10^6 m/s.

3.2. Interstroke Intervals

Interstroke intervals are calculated for all strokes in 47 MS +CG flashes. The distribution is shown in Figure 6a. Interstroke intervals have a very large range from 1.0 to 1,320.6 ms. However, it should be noted that the flash with the largest interstroke interval of 1,320.6 ms is actually a bipolar flash and will be analyzed in more detail. Except of this extreme value, all interstroke intervals are smaller than 470 ms, and from Figure 6a, we can see interstroke intervals are mainly smaller than 120 ms. The arithmetic mean (AM) and geometric mean (GM) of interstroke intervals are 122.2 and 64.4 ms when including the largest value and 103.2 and 61.4 ms when excluding the largest value. As summarized in Table 1, many other studies also reported the large range of interstroke intervals from several milliseconds to hundreds of milliseconds (Adhikari et al., 2016; Baharudin et al., 2016; Cooray & Pérez, 1994; Nag & Rakov, 2012; Qie et al., 2013). As for the mean values, the AM is easily influenced by extremely small or large values, so the GM is more appropriate to measure the average interstroke interval, and as summarized in Table 1, GM values in most studies are in the range of 50 to 100 ms. These results are generally similar to interstroke intervals for subsequent strokes in −CG flashes. For example, Cooray and Pérez (1994) reported that interstroke intervals of 568 subsequent strokes in 271 −CG flashes, without differentiating strokes creating new terminations, had an AM of 65 ms and a GM of

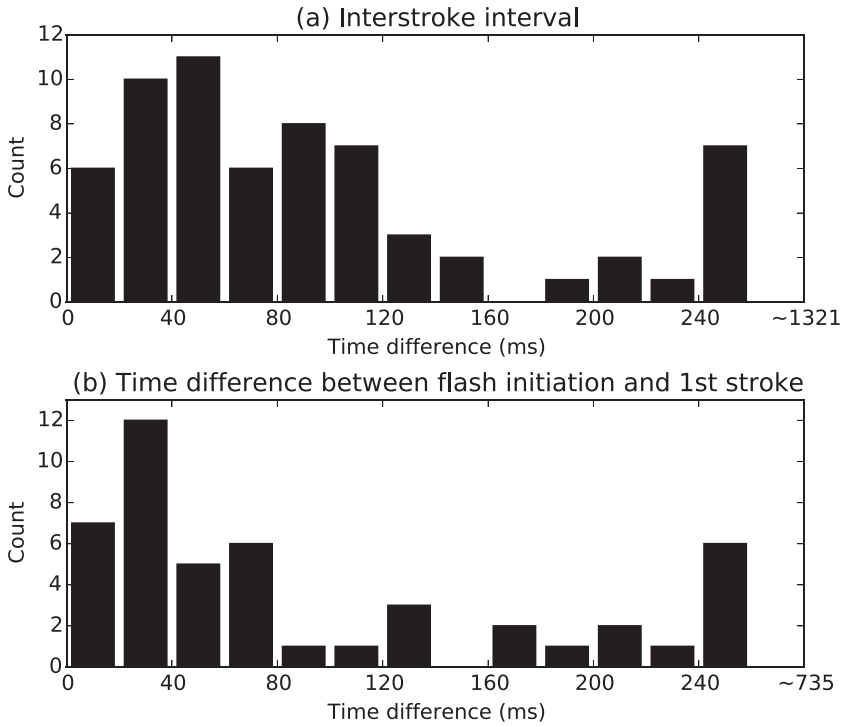

Figure 6. Distributions of (a) interstroke interval and (b) time difference between flash initiation and the first stroke in MS +CG flashes.

48 ms. Stolzenburg et al. (2019), based on high-speed video and *E* change records, reported that the mean and median values of interstroke intervals for 488 subsequent strokes were 87 and 65 ms, and among these subsequent strokes, 88 strokes producing new terminations had a mean value of interstroke interval of 94 ms.

As described above, the flash with the largest interstroke interval is a bipolar flash and is shown in Figure 7. Sources of this flash superimposed on the radar reflectivity are shown in Figure S7. The first and the second positive RSs are separated by 1,320.6 ms, but it is clear that there is also a negative RS between these two positive RSs. *E* change waveforms of the negative RS recorded by all sites are shown in Figure S8. It should be noted that the negative RS is located on the sea, so it is unlikely that the negative RS belongs to an upward flash triggered by the preceding positive RS. It is not clear whether the occurrence of the negative RS has contributed to the extremely long interval between the two positive RSs. The time difference between the negative RS and the second positive RS is 956.7 ms, still much larger than interstroke intervals in other MS +CG flashes. The duration and horizontal extent of this flash is also very large. The flash duration is about 2.2 s, and the horizontal extent is about 110 × 60 km. This flash is also special in that all three subsequent positive RSs are larger than the first RS, possibly due to the extremely long interstroke interval. From Figure 7b, it appears that leaders progressed with a velocity much slower than 1×10^5 m/s during the period between the first and the second positive RSs, implying that these leaders might be positive leaders. However, the overall low velocity was actually due to leaders propagating mainly in the tangential direction (the plot for this period is shown in Figure S9), and we believe the detected sources were mainly from negative leaders.

Interstroke intervals of several milliseconds in +CG flashes are also rarely reported. In this study, we observed three MS +CG flashes with interstroke intervals smaller than 2 ms (1.0, 1.3 and 1.8 ms). Interestingly, the horizontal distances between corresponding RSs are also very small (1.1, 2.7, and 3.2 km). As we will see in section 3.3, these strokes have smaller distances than most of other strokes. It is likely that these sequential strokes are produced when two branches of a positive leader connect to the ground sequentially, similar to the so-called "multiple termination stroke" in −CG flashes (e.g., Rakov & Uman, 1994; Sun et al., 2016). *E* change waveforms of two cases (interstroke intervals of 1.0 and 1.3 ms)

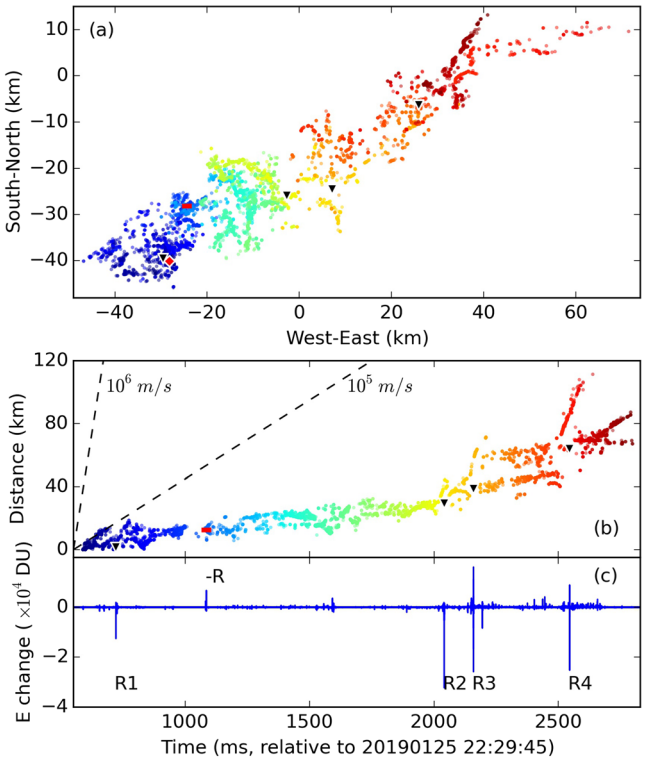

Figure 7. The +CG flash with the largest interstroke interval (1,032.6 ms) in this study. (a) Plan view. (b) Horizontal distance (relative to the initiation location) versus time. (c) *E* change waveform. The red diamond represents the initiation location. Black triangles represent positive RSs. Red minus sign represents the negative RS. The color scale of source points indicates the time corresponding to the time coordinate of Figure 7c. Slopes of two black dashed lines represent velocities of 10^5 and 10^6 m/s.

are shown in Figure 8. Interestingly, in both cases, the two strokes have some similar features. First, in both cases, the two strokes are subsequent strokes. Second, in both cases, the two strokes have similar peak amplitudes. Third, in both cases, waveforms of the two strokes have certain similarities, such as the pulse width.

We also calculated the time difference between the first positive RS and the flash initiation in 47 MS +CG flashes, and the distribution is shown in Figure 6b. We can see the distribution is generally similar to that of the interstroke interval. The time differences range from 6.7 to 734.5 ms. The AM and GM are 117.9 and 64.4 ms, respectively, also similar to those of interstroke intervals.

3.3. Horizontal Distances Between Sequential Return Strokes

Horizontal distances between sequential RSs (D_{RS}) in 47 MS +CG flashes are calculated, and the distribution is shown in Figure 9a. The value of D_{RS} ranges from 1.1 to 37.3 km. The AM and GM are 13.1 and 9.7 km, respectively. Only three studies so far provided distances between sequential RSs (Johari et al., 2017; Nag & Rakov, 2012; Saba et al., 2010), and results in this study are in general agreement with previous studies as summarized in Table 1.

It is interesting to note that distances between RSs in MS +CG flashes are generally larger than those between RSs creating new terminations in −CG flashes (Gao et al., 2019; Thottappillil et al., 1992). The difference is probably due to different origination mechanisms of leaders for subsequent strokes in +CG and −CG flashes. As will be discussed in section 4, most subsequent strokes in +CG flashes are likely initiated by positive leaders originating from in-cloud negative leader channels, so the distance between sequential positive strokes is approximately the distance traveled by a negative leader during the interstroke interval. On the other hand, subsequent RSs in −CG flashes are produced by recoil leaders propagating backward from positive leader channels to the initiation location and then deflecting from the previous main channel during the downward propagation (Gao et al., 2019; Stolzenburg et al., 2019). As a result, new terminations are usually very close to old terminations in −CG flashes.

It has long been postulated that subsequent strokes in +CG flashes cannot follow the same channel as a previous stroke (Mazur, 2002; Mazur & Ruhnke, 1993). However, video observations of MS +CG flashes have shown that some subsequent RSs in +CG flashes indeed followed a previously created channel (Fleenor et al., 2009; Saba et al., 2010), although such cases appear to be extremely rare. In this study, all subsequent strokes in +CG flashes created new terminations. The minimum horizontal distance between sequential positive RSs is 1.1 km. The two strokes also had the minimum interstroke interval. They have been analyzed in section 3.2, and their *E* change waveforms are shown in Figure 8a.

We also calculated horizontal distances between flash initiation location and the first positive RS (D_{ini}) for all MS +CG flashes, and the distribution is shown in Figure 9b. The value of D_{ini} ranges from 0.4 to 42.1 km. The AM and GM are 6.1 and 3.6 km, respectively, much smaller than those of D_{RS}. The difference is also clear by comparing Figures 9a and 9b. Although the maximum of D_{ini} is larger than that of D_{RS}, most values of D_{ini} are smaller than 8 km. By contrary, values of D_{RS} distribute relatively evenly from 0 to 32 km. The distinctly different distributions of D_{ini} and D_{RS} indicate different origination mechanisms of positive leaders responsible for first and subsequent strokes in +CG flashes. We will make further discussion in section 4.

3.4. Return Stroke Peak Amplitudes

In this section we analyze peak amplitudes of first and subsequent RSs in MS +CG flashes. In order to compare peak amplitudes of RSs measured at different distances and at different observation sites, peak

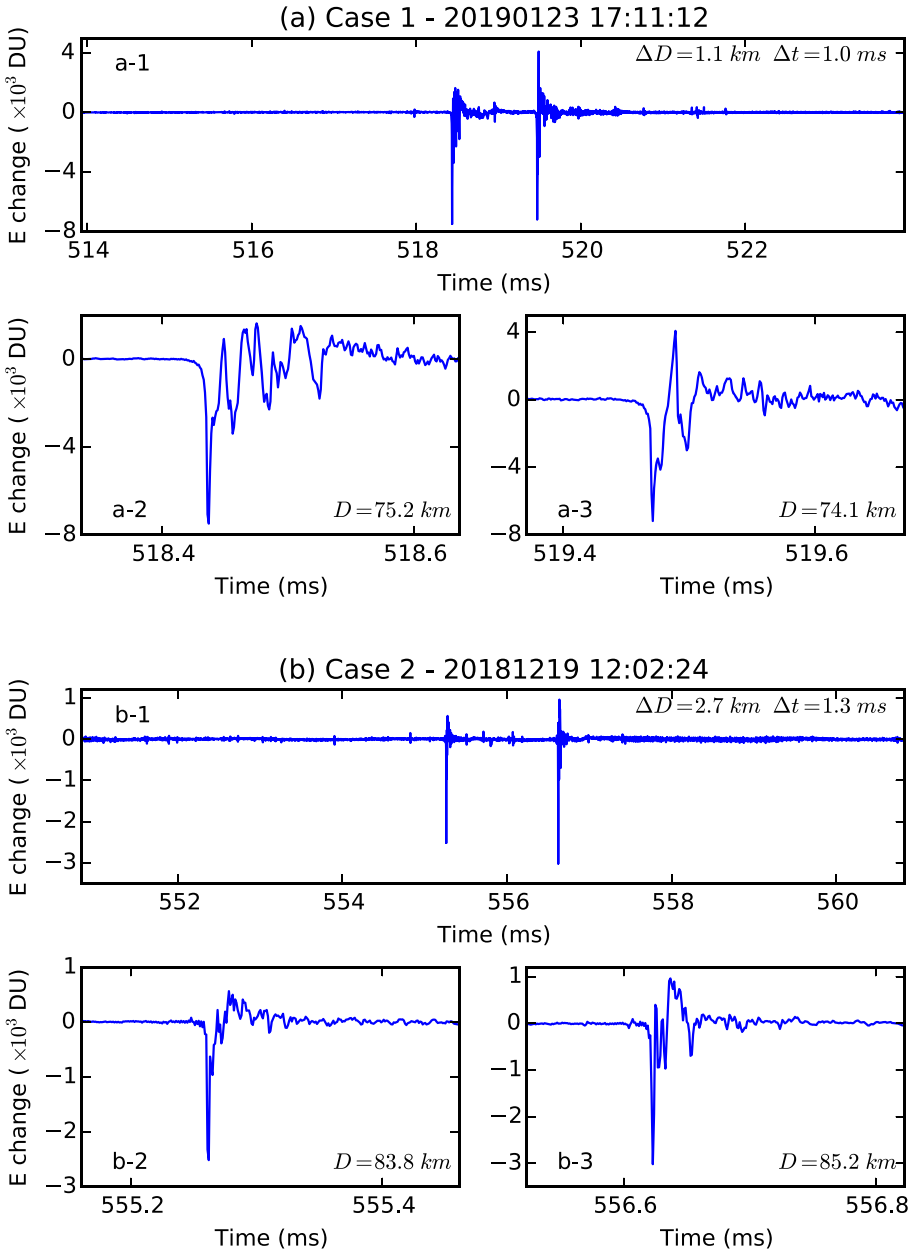

Figure 8. *E* change waveforms of sequential positive RSs with minimum time intervals (1.0 and 1.3 ms) in this study. The value of ΔD indicates the horizontal distance between two RSs. The value of Δt indicates the interstroke interval. The value of D indicates the distance between the stroke and the observation site recording the displayed waveform.

amplitudes are normalized to 100 km, and conversion coefficients between different sites are calculated. Details of the normalization and the conversion are described in Shi et al. (2019). Range-normalized peak amplitudes in the digital unit (DU) used for the following analyses are theoretically proportional to peak currents of RSs.

Figure 10 shows distributions of peak amplitudes of first and subsequent RSs in MS +CG flashes. We can see that first strokes are clearly much stronger than subsequent strokes. The mean value of first stroke peak amplitude is 13,321 DU and that of subsequent stroke amplitude is 6,021 DU. Subsequent stroke amplitudes are on average 0.45 of first stroke amplitudes. As summarized in Table 1, this result is smaller than those reported by Fleenor et al. (2009) and Saba et al. (2010) but is very close to those reported by Baharudin et al. (2016) and Johari et al. (2017).

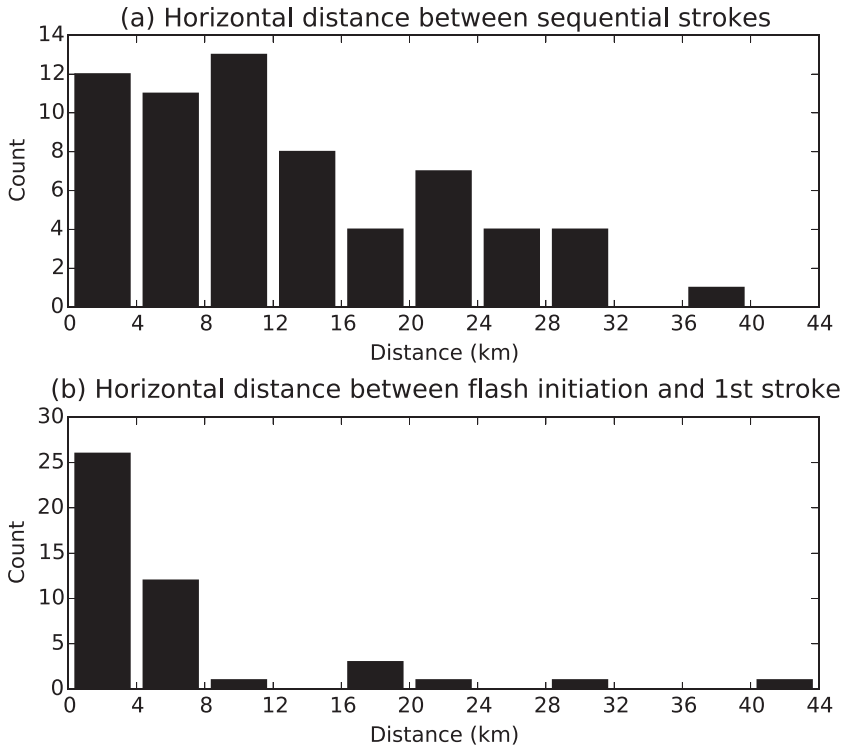

Figure 9. Distributions of (a) horizontal distances between sequential RSs and (b) horizontal distances between flash initiation location and the first RS.

For every MS +CG flash, the first stroke amplitude is compared to the amplitude of the largest subsequent stroke, and the result is shown in Figure 11a. In 39 flashes (83%), the first stroke is stronger than the largest subsequent stroke. These events are represented by blue bars in Figure 11a. For these events, the ratio of the first stroke amplitude to the strongest subsequent stroke amplitude is calculated, and the mean value is 3.0. In the remaining eight flashes (17%), the largest subsequent stroke is stronger than the first stroke. These events are represented by red bars in Figure 11a. For these events, the ratio of the strongest subsequent stroke amplitude to the first stroke amplitude is calculated, and the mean value is 2.0. This result indicates that first strokes in MS +CG flashes are usually much stronger than subsequent strokes. Similarly, first strokes in −CG flashes are also usually stronger than subsequent strokes, even when subsequent strokes create new terminations (Gao et al., 2019; Rakov & Uman, 1990).

For MS +CG flashes with at least three strokes, the amplitude of the nth ($n >= 2$) stroke is compared with that of the ($n + 1$)th stroke, and the result is shown in Figure 11b. There are nine strokes stronger than the following stroke (blue bars) and eight strokes stronger than the previous stroke (red bars), indicating that subsequent stroke amplitudes do not show any increasing or decreasing trend with the stroke order.

There have been reports that peak amplitudes of subsequent strokes in −CG flashes are associated with the time interval with the previous stroke (e.g., Diendorfer et al., 1998). Here we examine the relationship between subsequent stroke amplitudes in +CG flashes and time differences with the previous stroke, and the result is shown in Figure 12a. Note that the maximum interstroke interval of 1,320.6 ms (Figure 7) is not shown in Figure 12a. Figure 12a shows a weak positive correlation between interstroke intervals and peak amplitudes with the correlation coefficient of 0.29. If we exclude strokes with interstroke intervals larger than 300 ms, the correlation coefficient increases to 0.48. Figure 12b shows the relationship between peak amplitudes and distances with previous strokes, and it is clear that the correlation is much weaker. These results indicate that peak amplitudes of subsequent strokes in +CG flashes are more closely associated with time differences with previous strokes, especially when the time difference is not too large. It should be noted that strokes in +CG flashes normally do not follow a previous RS channel, so the reason of the

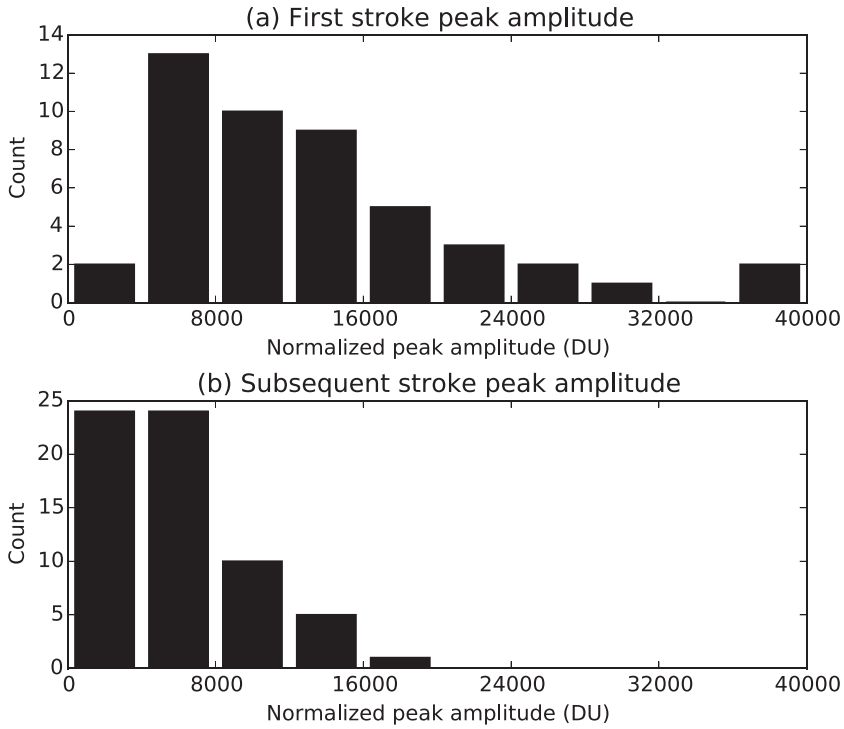

Figure 10. Distributions of normalized peak amplitudes of first and subsequent RSs in MS +CG flashes.

correlation is different from that for strokes in −CG flashes. One possible explanation is that different strokes in the same +CG flash, although they do not share the same channel, lower positive charges from the same charge region, so the longer the time difference is, the larger the amount of charges built up by updrafts and available for the next stroke, and thus, the stronger the subsequent stroke is. Additionally, during stroke intervals, as in-cloud negative leaders keep extending in the positive charge region, more and more positive charges may be induced on the leader system, which may also contribute to stronger subsequent strokes.

As analyzed previously, in eight MS +CG flashes, the largest subsequent stroke is stronger than the first stroke. In these eight flashes, there is a total of 10 subsequent strokes stronger than the corresponding first strokes. These 10 subsequent strokes are represented by red points in Figure 12. For nine strokes (the one with the largest interstroke interval is not shown in Figures 12a and 12c), the interstroke interval is larger than 100 ms. As analyzed in section 3.2, the GM of interstroke interval is only 64.4 ms. This result is in agreement with the correlation between peak amplitudes and interstroke intervals analyzed above.

4. Inferences on Origins of Positive Leaders for First and Subsequent Strokes in +CG Flashes

Due to the rarity of +CG flashes and the low radiation power in radio frequencies produced by positive leaders (e.g., Shao et al., 1999), it is very difficult to obtain direct evidence on how positive leaders initiating positive RSs originate in thunderclouds (Li et al., 2020). Various scenarios for the origination of positive leaders initiating first positive strokes were discussed by van der Velde et al. (2014) based on the bidirectional leader concept and the lightning mapping array observation. Possible charge configurations responsible for the production of +CG flashes were also discussed by Nag and Rakov (2012). Some of the scenarios proposed by these studies also seem to be applicable for the origination of positive leaders initiating subsequent positive strokes, and these scenarios will be examined in this section.

The first scenario is similar to the scenario "f" in Nag and Rakov (2012). Assuming an in-cloud positive leader propagates forward, one branch turns to the ground and initiates an RS, while the main channel keeps propagating forward. Later, another branch develops from the channel, propagates to the ground, and

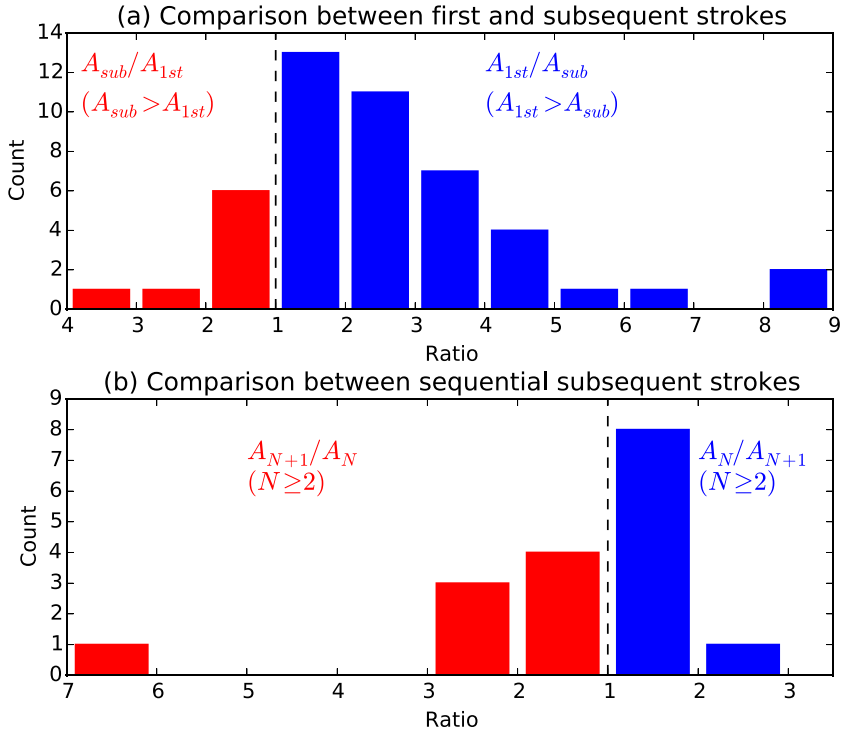

Figure 11. (a) Comparison between the amplitude of the first stroke (A_{1st}) and the amplitude of the largest subsequent stroke (A_{sub}) in the same +CG flash. Blue bars represent events with larger A_{1st}, and red bars represent events with larger A_{sub}. (b) Comparison between sequential subsequent strokes for +CG flashes with at least three positive strokes. Blue bars represent events with the amplitude of the Nth stroke (A_N) larger than that of the following stroke (A_{N+1}). Red bars represent events with larger A_{N+1} than A_N.

initiates a subsequent stroke. In this scenario, the minimum required velocity of the positive leader roughly equals to the horizontal distance between the two strokes divided by the interstroke interval. To examine this scenario, the scatterplot of horizontal distances between sequential strokes versus interstroke intervals is shown in Figure 12c. We can see that for most of subsequent strokes, the distance and the time interval correspond to a velocity value in the range of 0.5 to 5×10^5 m/s. In other words, for most MS +CG flashes, the in-cloud leader connecting sequential RS channels should have a velocity larger than 0.5×10^5 m/s. However, as demonstrated by Wu et al. (2019), velocities of in-cloud positive leaders are mainly in the range of 1 to 3×10^4 m/s. Although Wu et al. (2019) only analyzed positive leaders in intracloud (IC) and −CG flashes, it is likely that in-cloud horizontal positive leaders in +CG flashes are generally similar to those in IC and −CG flashes. Therefore, the scenario that multiple branches of a positive leader channel produce multiple positive RSs does not seem to be applicable to most of cases.

The second scenario is that positive leaders initiating subsequent strokes originate from in-cloud negative leader channels with current cutoff, similar to the scenario "e" in Nag and Rakov (2012) and the scenario 5 in van der Velde et al. (2014). After the first positive stroke, in-cloud negative leaders keep propagating. When the current cutoff occurs in a negative leader, a new positive leader may develop from the negative leader channel and may initiate a subsequent positive stroke. Observations of positive RSs preceded by extensive IC discharges (Kong et al., 2008; Saba et al., 2009) also agree with this scenario. In this scenario, it is the negative leader that traverses the distance between two sequential positive strokes, so it is in agreement with the relationship between horizontal distances and interstroke intervals in Figure 12c.

In order to further examine this scenario, we analyze the distance-time relationship for sources before and after each subsequent strokes similar to the analysis made by van der Velde et al. (2014). Results for six subsequent strokes are shown in Figure 13. In all subplots in Figure 13, the stroke under consideration is represented by a black cross sign at (0, 0). The blue, yellow, and red dashed lines represent velocities of 2×10^4, 1×10^5, and 1×10^6 m/s, respectively. For the strokes in Figures 13a–13d, a negative leader first approaching

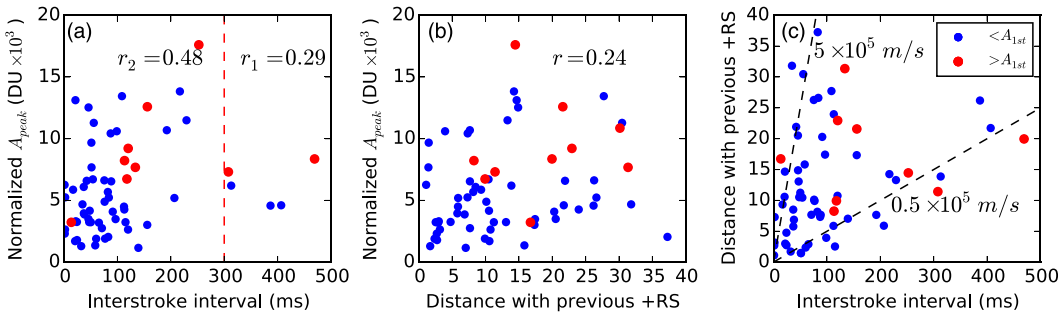

Figure 12. Relationships among normalized peak amplitudes of subsequent strokes in +CG flashes, interstroke intervals, and distances with previous positive strokes. Red points represent subsequent strokes stronger than corresponding first strokes. A stroke with extremely large time difference (1,321 ms) is not shown in Figures 12a and 12c. Correlation coefficient r_1 is for all events in Figure 12a. Correlation coefficient r_2 is for events on the left of the red dashed line. Slopes of two black dashed lines in Figure 12c represent velocities of 5×10^5 and 0.5×10^5 m/s.

the location of the positive stroke and then propagating away can be recognized. The distance between the negative leader and the stroke decreases to near 0 at some tens of milliseconds before the stroke. These cases are in perfect agreement with the notion that positive leaders for subsequent strokes initiate from in-cloud negative leader channels. It seems very likely that a positive leader develops from the point on the negative leader channel that is very close (near 0) to the location of the positive stroke and after tens of milliseconds the positive leader reaches the ground and initiates a positive RS. We examined all 64 subsequent positive strokes in this study and found that at least 37 strokes are preceded by similar negative leaders. Twenty-two more examples are shown in Figures S10–S12 and S13a–S13d. The distance-time plots for all strokes are provided in the data repository (see Acknowledgments section). Excluding some subsequent strokes with extremely small time differences from previous strokes (Figure 8) and also considering the fact that in some cases the location results are not good enough to make a correct determination of the processes before the positive strokes, we believe that for most subsequent strokes in MS +CG flashes, positive leaders originate from in-cloud negative channels. This conclusion is also consistent with the recent observation of a MS +CG flash by Yuan et al. (2020).

However, details on how positive leaders develop from negative leader channels are not clear. In the scenario "e" proposed by Nag and Rakov (2012) and the scenario 5 proposed by van der Velde et al. (2014), the current cutoff of the in-cloud negative leader is needed for a new positive leader to develop. According to van der Velde et al. (2014), the new positive leader develops from the point on the old negative leader where the current cutoff occurs. In other words, the current cutoff occurs at the point of the negative leader very close to the location of the positive stroke. It is impossible for the current cutoff to occur right after the negative leader passes the point; the negative leader needs to continue developing forward for a while before the current cutoff occurs. However, according to Figures 13a–13d, the time difference between the positive stroke and the moment when the distance is near 0 is only tens of milliseconds, which seems to be too short for the current cutoff to occur and for the new positive leader to start and to develop to the ground. Additionally, the short time difference indicates that the current cutoff occurs at a point not very far away from the head of the developing negative leader, which is somewhat difficult to explain as it is expected that the current cutoff tends to occur at a relatively old part of the leader with reduced conductivity.

An alternative mechanism to explain the positive leader developing from the negative leader channel is similar to the polarity reversal mechanism proposed by Wang and Takagi (2008) and Shi et al. (2018). Suppose a branch of the negative leader, which is not well resolved by the location results, becomes defunct while the main channel keeps propagating forward, positive charges from the head of the main channel may be transferred back to the defunct branch. When enough positive charges are transferred to the branch, a new positive leader may be triggered, and it may develop to the ground and initiate a positive stroke. In this mechanism, the head of the defunct branch corresponds to the point with 0 distance in Figures 13a–13d. This mechanism is also consistent with the report by Yuan et al. (2020) that a positive leader initiated from a decayed negative leader branch.

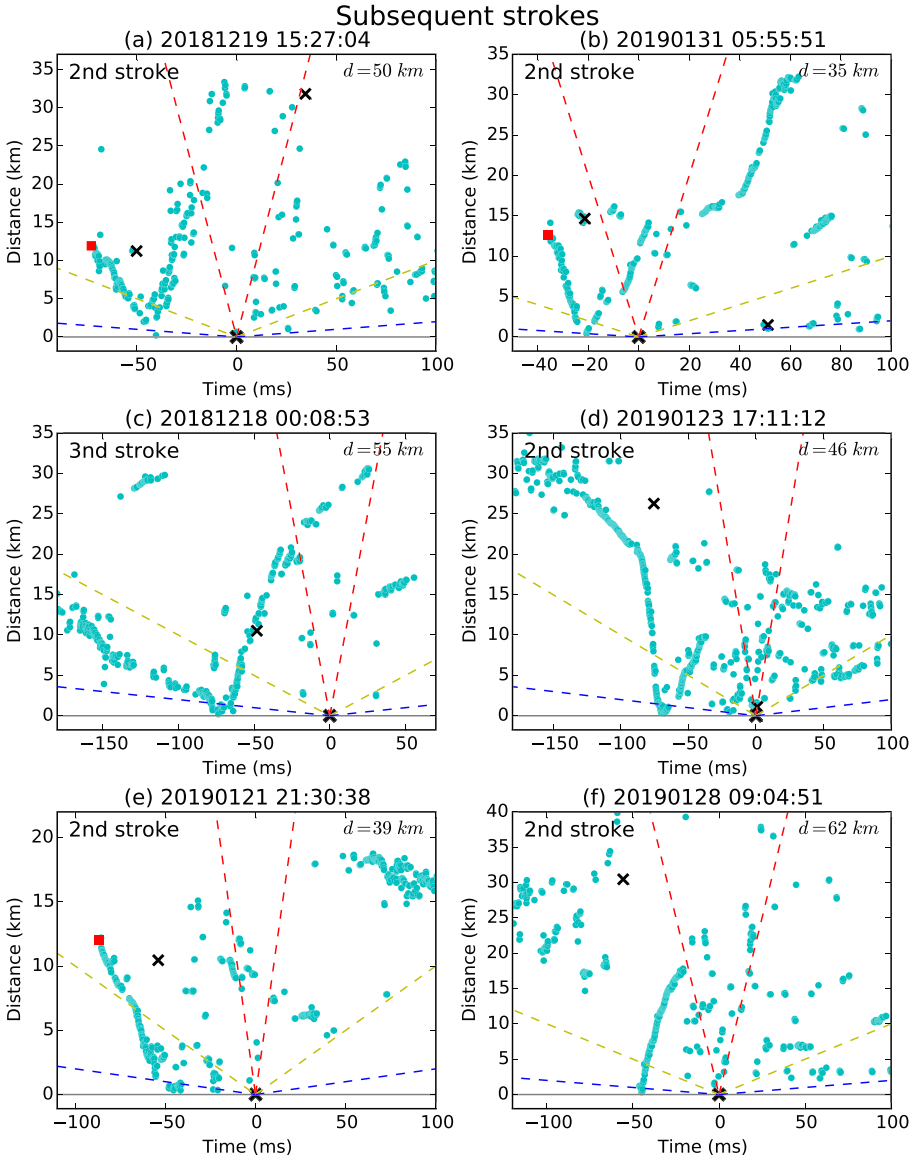

Figure 13. The scatterplot of the distance versus time for sources before and after some subsequent positive RSs. The distance and the time are calculated relative to the stroke shown at (0, 0). Black crosses not at (0, 0) are other positive RSs in the same flash. The red square, if shown, is the first source of the +CG flash. The blue, yellow, and red dashed lines represent velocities of 2×10^4, 1×10^5, and 1×10^6 m/s, respectively. The value of d indicates the distance between the stroke at (0, 0) and the center of the FALMA network in Figure 1.

Apart from the characteristic V-shaped distance-time plots in Figures 13a–13d, we found two cases in which a negative leader can be seen approaching the location of the positive stroke but it just stops and does not propagate away. One example is shown in Figure 13e, and the other is shown in Figure S13e. In these cases, positive leaders for subsequent strokes may develop from the head of decayed negative leader channels. In another two cases shown in Figures 13f and S13f, only a negative leader propagating away from the location of the positive stroke can be recognized. These cases may be similar to the scenario 4 in van der Velde et al. (2014), that is, the positive leader is initiated together with the negative leader by a new bidirectional development. These special cases seem to be relatively rare for subsequent positive strokes.

The origination mechanism of positive leaders for first positive strokes seems to be varied and complicated as demonstrated by van der Velde et al. (2014). If we compare Figures 9a and 9b, we can see that the distance

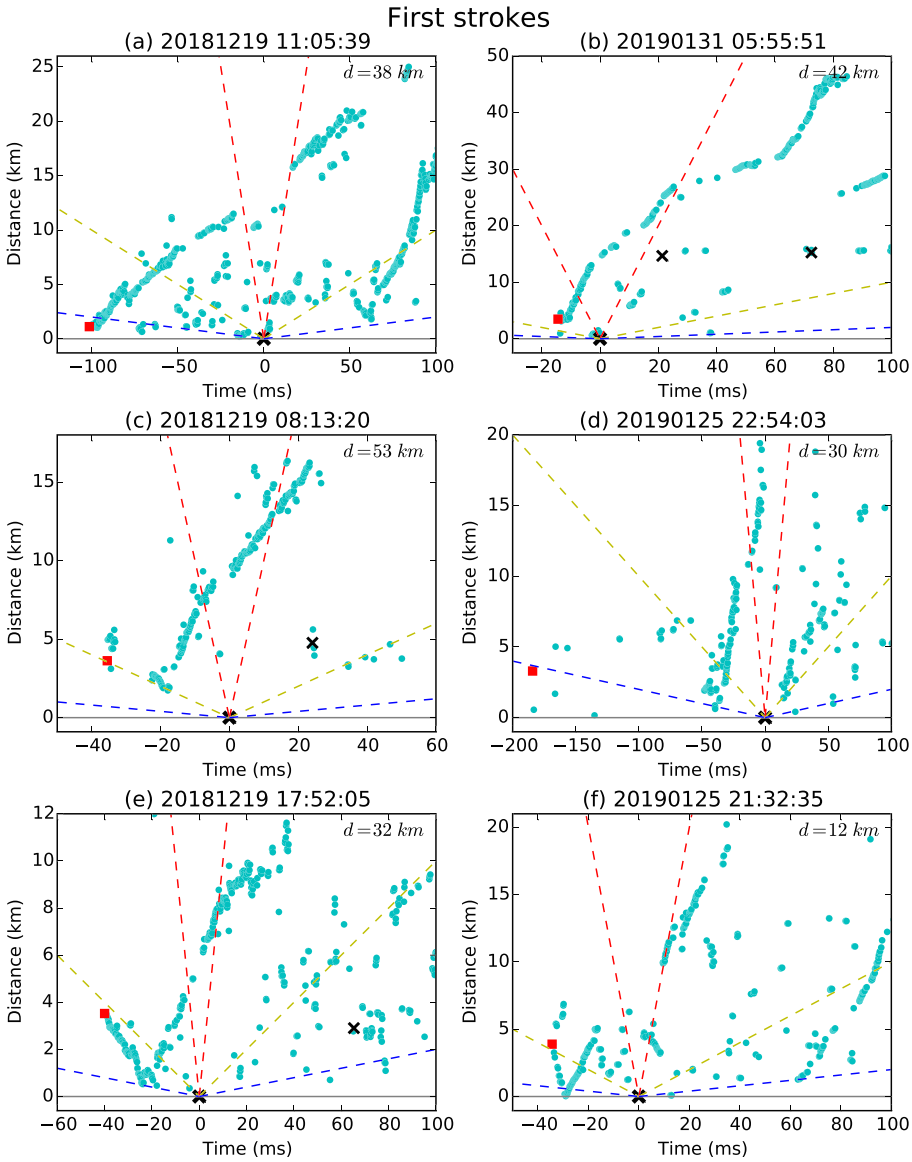

Figure 14. The same as Figure 13 but for six first RSs in MS +CG flashes.

between the first stroke and the flash initiation location (D_{ini}) is usually much smaller than the distance between sequential strokes (D_{RS}). This result indicates that the origination mechanism of positive leaders for first strokes is usually different from that for subsequent strokes. However, even for first strokes with very small D_{ini} (<5 km), different mechanisms seem to be necessary. The distance-time plots for six first strokes are shown in Figure 14. Plots for other first strokes can be found in the data repository. For the strokes in Figures 14a and 14b, we can see in each case the flash starts with a negative leader propagating away from the location of the positive stroke, indicating that a positive leader starting together as the negative leader goes directly down to the ground and initiates the first stroke. This mechanism is similar to the scenario 1 or 2 in van der Velde et al. (2014). For the strokes in Figures 14c and 14d, some sources are located before the initiation of a negative leader propagating away, and it is likely that the positive leader initiating the first stroke starts together as the negative leader sometime after the initiation of the flash. This mechanism may be similar to the scenario 4 in van der Velde et al. (2014) and also similar to the mechanism for the subsequent stroke in Figure 13f. First strokes in Figures 14e and 14f are somewhat similar to the subsequent strokes in Figures 13a–13d. It is possible that the positive leader initiating the

first stroke starts from the point on the negative leader channel that is very close to the positive stroke location, but we cannot rule out the possibility that the positive leader simply starts together with the negative leader at the beginning of the flash.

In summary, it is inferred that for the majority of MS +CG flashes analyzed in this study, positive leaders initiating subsequent strokes mainly originated from in-cloud negative leader channels, but origination mechanisms for positive leaders initiating first positive strokes seem to be more varied and complicated.

5. Conclusion

During the winter observation in the Hokuriku region of Japan, we successfully recorded 47 MS +CG flashes, which were imaged by the FALMA consisting of 14 sites. With this high-quality data set, various characteristics of MS +CG flashes are analyzed. Major findings are summarized as follows.

MS +CG flashes observed in this study include 34 two-stroke flashes, 10 three-stroke flashes, 2 four-stroke flashes, and 1 five-stroke flashes. We also observed 216 single-stroke flashes. The percentage of MS +CG flashes is 17.9%, and the mean multiplicity of +CG flashes is 1.24.

Interstroke intervals range from 1.0 to 1,320.6 ms with the AM and GM of 122.2 and 64.4 ms. The flash with the maximum interstroke interval is actually a bipolar flash. Excluding this flash, the maximum interstroke interval is 469.2 ms, and the AM and GM are 103.2 and 61.4 ms. Interstroke intervals smaller than 2 ms are observed in three flashes. Corresponding RSs also have small horizontal distances, indicating that they may be produced by two branches of the same positive leader, similar to the so-called "multiple termination stroke" in −CG flashes.

Horizontal distances between sequential positive RSs range from 1.1 to 37.3 km with the AM and GM of 13.1 and 9.7 km. No subsequent strokes were found to strike at the same location as a previous stroke. Horizontal distances between sequential positive RSs are usually much larger than distances between first positive RSs and lightning initiation locations.

Subsequent stroke peak amplitudes are on average 0.45 of first stroke peak amplitudes. In 39 flashes (83.0%), the first stroke is found to be stronger than the largest subsequent stroke. For subsequent strokes, peak amplitudes do not seem to depend on the stroke order. Subsequent stroke amplitudes are weakly correlated with preceding interstroke intervals.

Various scenarios for the origination of positive leaders initiating subsequent strokes in MS +CG flashes are examined. For most subsequent strokes, a negative leader first approaching and getting very close to the location of the positive stroke tens of milliseconds before the positive stroke and then propagating away can be recognized. This result indicates that positive leaders initiating subsequent strokes mainly originate from in-cloud negative leader channels. On the other hand, the origination mechanism of positive leaders initiating first strokes seems to be more varied and complicated, in agreement with previous studies.

Data Availability Statement

Data of all positive strokes analyzed in this paper and distance-time plots (section 4) for all positive strokes can be downloaded online (http://doi.org/10.5281/zenodo.3937501).

Acknowledgments
This work was supported by the Ministry of Education, Culture, Sports, Science, and Technology of Japan (Grants 16H04315, 18K13618, and 20H02129). The authors thank Oscar van der Velde and two anonymous reviewers for their valuable comments, which helped improve the quality of this paper.

References

Adhikari, P. B., Sharma, S., & Baral, K. (2016). Features of positive ground flashes observed in Kathmandu Nepal. *Journal of Atmospheric and Solar-Terrestrial Physics*, *145*, 106–113. https://doi.org/10.1016/j.jastp.2016.04.016

Baharudin, Z. A., Cooray, V., Rahman, M., Hettiarachchi, P., & Ahmad, N. A. (2016). On the characteristics of positive lightning ground flashes in Sweden. *Journal of Atmospheric and Solar-Terrestrial Physics*, *138–139*, 106–111. https://doi.org/10.1016/j.jastp.2015.12.014

Cooray, V., & Pérez, H. (1994). Some features of lightning flashes observed in Sweden. *Journal of Geophysical Research*, *99*(D5), 10,683–10,688. https://doi.org/10.1029/93JD02366

Diendorfer, G., Schultz, W., & Rakov, V. A. (1998). Lightning characteristics based on data from the Austrian lightning locating system. *IEEE Transactions on Electromagnetic Compatibility*, *40*(4), 452–464. https://doi.org/10.1109/15.736206

Fleenor, S. A., Biagi, C. J., Cummins, K. L., Krider, E. P., & Shao, X. M. (2009). Characteristics of cloud-to-ground lightning in warm-season thunderstorms in the Central Great Plains. *Atmospheric Research*, *91*(2–4), 333–352. https://doi.org/10.1016/j.atmosres.2008.08.011

Gao, P., Wang, D., Shi, D., Wu, T., & Takagi, N. (2019). Characterization of multitermination CG flashes using a 3D Lightning Mapping System (FALMA). *Atmosphere*, *10*, 625. https://doi.org/10.3390/atmos10100625

Hazmi, A., Emeraldi, P., Hamid, M. I., Takagi, N., & Wang, D. (2017). Characterization of positive cloud to ground flashes observed in Indonesia. *Atmosphere*, *8*, 4. https://doi.org/10.3390/atmos8010004

Heidler, F., & Hopf, C. (1998). Measurement results of the electric fields in cloud-to-ground lightning in nearby Munich, Germany. *IEEE Transactions on Electromagnetic Compatibility*, *40*(4), 436–443. https://doi.org/10.1109/15.736204

Johari, D., Cooray, V., Rahman, M., Hettiarachchi, P., & Ismail, M. M. (2017). Features of the first and the subsequent return strokes in positive ground flashes based on electric field measurements. *Electric Power Systems Research*, *150*, 55–62. https://doi.org/10.1016/j.epsr.2017.04.031

Kong, X., Qie, X., & Zhao, Y. (2008). Characteristics of downward leader in a positive cloud-to-ground lightning flash observed by high-speed video camera and electric field changes. *Geophysical Research Letters*, *35*, L05816. https://doi.org/10.1029/2007GL032764

Lang, T. J., Pédeboy, S., Rison, W., Cerveny, R. S., Cerveny, R. S., Montanyà, J., et al. (2017). WMO world record lightning extremes: Longest reported flash distance and longest reported flash duration. *Bulletin of the American Meteorological Society*, *98*(6), 1153–1168. https://doi.org/10.1175/BAMS-D-16-0061.1

Li, D., Azadifar, M., Rachidi, F., Rubinstein, M., Diendorfer, G., Sheshyekani, K., et al. (2016). Analysis of lightning electromagnetic field propagation in mountainous terrain and its effects on ToA-based lightning location systems. *Journal of Geophysical Research: Atmospheres*, *121*, 895–911. https://doi.org/10.1002/2015JD024234

Li, S., Qiu, S., Shi, L., & Li, Y. (2020). Broadband VHF observations of two natural positive cloud-to-ground lightning flashes. *Geophysical Research Letters*, *47*, e2019GL086915. https://doi.org/10.1029/2019GL086915

Lyons, W. A., Bruning, E. C., Warner, T. A., MacGorman, D. R., Edgington, S., Tillier, C., & Mlynarczyk, J. (2020). Megaflashes: Just how long can a lightning discharge get? *Bulletin of the American Meteorological Society*, *101*(1), E73–E86. https://doi.org/10.1175/BAMS-D-19-0033.1

Lyons, W. A., Uliasz, M., & Nelson, T. E. (1998). Large peak current cloud-to-ground lightning flashes during the summer months in the contiguous United States. *Monthly Weather Review*, *126*(8), 2217–2233. https://doi.org/10.1175/1520-0493(1998)126<2217:LPCCTG>2.0.CO;2

Mazur, V. (2002). Physical processes during development of lightning flashes. *Comptes Rendus Physique*, *3*(10), 1393–1409. https://doi.org/10.1016/S1631-0705(02)01412-3

Mazur, V., & Ruhnke, L. H. (1993). Common physical processes in natural and artificially triggered lightning. *Journal of Geophysical Research*, *98*(D7), 12,913–12,930. https://doi.org/10.1029/93JD00626

Nag, A., & Rakov, V. A. (2012). Positive lightning: An overview, new observations, and inferences. *Journal of Geophysical Research*, *117*, D08109. https://doi.org/10.1029/2012JD017545

Qie, X., Wang, Z., Wang, D., & Liu, M. (2013). Characteristics of positive cloud-to-ground lightning in Da Hinggan Ling forest region at relatively high latitude, northeastern China. *Journal of Geophysical Research: Atmospheres*, *118*, 13,393–13,404. https://doi.org/10.1002/2013JD020093

Qie, X., Yu, Y., Wang, D., Wang, H., & Chu, R. (2002). Characteristics of cloud-to-ground lightning in Chinese inland plateau. *Journal of the Meteorological Society of Japan*, *80*(4), 745–754. https://doi.org/10.2151/jmsj.80.745

Rakov, V. A. (2003). A review of positive and bipolar lightning discharges. *Bulletin of the American Meteorological Society*, *84*(6), 767–776. https://doi.org/10.1175/BAMS-84-6-767

Rakov, V. A., & Uman, M. A. (1990). Some properties of negative cloud-to-ground lightning flashes versus stroke order. *Journal of Geophysical Research*, *95*(D5), 5447–5453. https://doi.org/10.1029/JD095iD05p05447

Rakov, V. A., & Uman, M. A. (1994). Origin of lighting electric field signatures showing two return-stroke waveforms separated in time by a millisecond or less. *Journal of Geophysical Research*, *99*(D4), 8157–8165. https://doi.org/10.1029/94JD00165

Saba, M. M. F., Campos, L. Z. S., Krider, E. P., & Pinto, O. Jr. (2009). High-speed video observations of positive ground flashes produced by intracloud lightning. *Geophysical Research Letters*, *36*, L12811. https://doi.org/10.1029/2009GL038791

Saba, M. M. F., Schulz, W., Warner, T. A., Campos, L. Z. S., Schumann, C., Krider, E. P., et al. (2010). High-speed video observations of positive lightning flashes to ground. *Journal of Geophysical Research*, *115*, D24201. https://doi.org/10.1029/2010JD014330

Schultz, C. J., Lang, T. J., Bruning, E. C., Calhoun, K. M., Harkema, S., & Curtis, N. (2018). Characteristics of lightning within electrified snowfall events using lightning mapping arrays. *Journal of Geophysical Research: Atmospheres*, *123*, 2347–2367. https://doi.org/10.1002/2017JD027821

Shao, X. M., Rhodes, C. T., & Holden, D. N. (1999). RF radiation observations of positive cloud-to-ground flashes. *Journal of Geophysical Research*, *104*(D8), 9601–9608. https://doi.org/10.1029/1999JD900036

Shi, D., Wang, D., Wu, T., & Takagi, N. (2019). Correlation between the first return stroke of negative CG lightning and its preceding discharge processes. *Journal of Geophysical Research: Atmospheres*, *124*, 8501–8510. https://doi.org/10.1029/2019JD030593

Shi, D., Wang, D., Wu, T., Thomas, R. J., Edens, H. E., Rison, W., et al. (2018). Leader polarity-reversal feature and charge structure of three upward bipolar lightning flashes. *Journal of Geophysical Research: Atmospheres*, *123*, 9430–9442. https://doi.org/10.1029/2018JD028637

Soula, S., van der Velde, O., Palmiéri, J., Chanrion, O., Neubert, T., Montanyà, J., et al. (2010). Characteristics and conditions of production of transient luminous events observed over a maritime storm. *Journal of Geophysical Research*, *115*, D16118. https://doi.org/10.1029/2009JD012066

Stolzenburg, M., Marshall, T. C., & Karunarathne, S. (2019). Inception of subsequent stepped leaders in lightning. *Meteorology and Atmospheric Physics*, *132*(4), 489–514. https://doi.org/10.1007/s00703-019-00702-8

Sun, Z., Qie, X., Liu, M., Jiang, R., Wang, Z., & Zhang, H. (2016). Characteristics of a negative lightning with multiple-ground terminations observed by a VHF lightning location system. *Journal of Geophysical Research: Atmospheres*, *121*, 413–426. https://doi.org/10.1002/2015JD023702

Thottappillil, R., Rakov, V. A., Uman, M. A., Beasley, W. H., Master, M. J., & Shelukhin, D. V. (1992). Lightning subsequent-stroke electric field peak greater than the first stroke peak and multiple ground terminations. *Journal of Geophysical Research*, *97*(D7), 7503–7509. https://doi.org/10.1029/92JD00557

van der Velde, O. A., & Montanyà, J. (2013). Asymmetries in bidirectional leader development of lightning flashes. *Journal of Geophysical Research: Atmospheres*, *118*, 13,504–13,519. https://doi.org/10.1002/2013JD020257

van der Velde, O. A., Montanyà, J., Soula, S., Pineda, N., & Mlynarczyk, J. (2014). Bidirectional leader development in sprite-producing positive cloud-to-ground flashes: Origins and characteristics of positive and negative leaders. *Journal of Geophysical Research: Atmospheres*, *119*, 12,755–12,779. https://doi.org/10.1002/2013JD021291

Wang, D., & Takagi, N. (2008). Characteristics of upward bipolar lightning derived from simultaneous recording of electric current and electric field change, Paper presented at the XXIX General Assembly, Int. Union of Radio Sci., Chicago, Ill.

Williams, E. R., Downes, E., Boldi, R., Lyons, W., & Hechman, S. (2007). Polarity asymmetry of sprite-producing lightning: A paradox. *Radio Science*, *42*, RS2S17. https://doi.org/10.1029/2006RS003488

Wu, T., Wang, D., & Takagi, N. (2018a). Locating preliminary breakdown pulses in positive cloud-to-ground lightning. *Journal of Geophysical Research: Atmospheres*, *123*, 7989–7998. https://doi.org/10.1029/2018JD028716

Wu, T., Wang, D., & Takagi, N. (2018b). Lightning mapping with an array of fast antennas. *Geophysical Research Letters*, *45*, 3698–3705. https://doi.org/10.1002/2018GL077628

Wu, T., Wang, D., & Takagi, N. (2019). Velocities of positive leaders in intracloud and negative cloud-to-ground lightning flashes. *Journal of Geophysical Research: Atmospheres*, *124*, 9983–9995. https://doi.org/10.1029/2019JD030783

Wu, T., Wang, D., & Takagi, N. (2020). A negative cloud-to-ground lightning flash initiating at a high altitude and starting without classic preliminary breakdown pulses. *Journal of Atmospheric Electricity.*, *39*(1), 16–32. https://doi.org/10.1541/jae.39.16

Yuan, S., Qie, X., Jiang, R., Wang, D., Sun, Z., Srivastava, A., & Williams, E. (2020). Origin of an uncommon multiple-stroke positive cloud-to-ground lightning flash with different terminations. *Journal of Geophysical Research: Atmospheres*, *125*, e2019JD032098. https://doi.org/10.1029/2019JD032098